

Scanning Tunneling Microscopy of Molecular Adsorbates at the Liquid–Solid Interface: Functional Group Variations in Image Contrast[†]

Leanna Giancarlo, Donna Cyr,[‡] Karen Muyskens,[§] and George W. Flynn*

Department of Chemistry and Columbia Radiation Laboratory, Columbia University,
New York, New York 10027

Received July 3, 1997. In Final Form: August 27, 1997

Recent studies have demonstrated that functionalized portions of long-chain hydrocarbons ($\text{CH}_3(\text{CH}_2)_n\text{X}$, where $\text{X} = \text{SH}, \text{S}, \text{SS}, \text{NH}_2, \text{Br}, \text{I}$) physisorbed on graphite at the liquid–solid interface exhibit enhanced contrast (increased tunneling current) when imaged by scanning tunneling microscopy (STM). The tunneling mechanism for such molecules can be investigated by examining the interplay between topographic and electronic structure/coupling factors. Utilizing a scanning tunneling spectroscopy methodology, changes in the STM images of two-dimensional thin films of amide-, bromide-, and sulfide-derivatized molecules have been observed as a function of applied bias voltage. For octadecanamide, the relative topographic height (increased tunneling probability) of the functional group compared to that of the hydrocarbon backbone peaks at $|V| = 1.4 \text{ V}$; this differs greatly from the voltage dependence obtained for docosane bromide, where the measured relative topographic height of the bromide end group remains constant for all voltages sampled. These trends are discussed in terms of the geometry of the molecular adsorbate and its electronic coupling to the substrate.

I. Introduction

While scanning tunneling microscopy (STM) has become a widely used tool to obtain atomically resolved images of surfaces under a variety of conditions, e.g. ultrahigh vacuum,^{1,2} ambient environments,^{3–5} electrochemical solutions,^{6–8} etc., there remains much debate regarding the mechanism by which adsorbates on surfaces appear “visible” to STM. In particular, the determination of the nature of the image contrast observed for electrically insulating adsorbates, such as substituted, long-chain hydrocarbons imaged at the liquid–solid interface, persists as an area of active research. In this paper, the voltage dependence of STM images of several thin films comprised of functionalized hydrocarbons physisorbed on graphite is examined. The motivation behind these studies lies in

providing information concerning the tunneling mechanism responsible for the enhanced contrast at the position of the functional group within the molecule. Primarily, we hope to elucidate the roles that *geometry*, as manifested by the spatial overlap between the STM probe and the functional group, and *electronic structure*, the coupling between the energy levels of the adsorbate and the surface Fermi level, play in the enhanced contrast or measured topographic height exhibited by certain functional groups.

Previous STM studies have examined changes in topographic images produced by systematically varying the functional groups in hydrocarbons adsorbed on graphite ($\text{CH}_3(\text{CH}_2)_n\text{X}$, where $\text{X} = \text{CH}_3, \text{OH}, \text{SH}, \text{S}, \text{SS}, \text{NH}_2, \text{Cl}, \text{Br}$, and I and $n = 17–29$).^{9–11} In addition to distinguishing between molecules on the basis of adsorbate–substrate and adsorbate–adsorbate interactions, as reflected in their two-dimensional packing arrangements, chemically distinct regions of the molecules have been differentiated by substituting functional groups at various positions along the carbon chain. For example, topographs of hydrocarbons with CH_3 , OH , or Cl terminal groups revealed little contrast variation between the derivatized atom or group of atoms and the hydrocarbon backbone; however, NH_2 , SH , Br , I , S , and SS demonstrate increased tunneling compared to the backbone, as evidenced by bright areas in the constant-current images.^{9–11}

On the basis of these experimental results, an empirical relationship has been proposed correlating the increasing tunneling current (higher tunneling probability) of the derivatized part of the molecule with increasing molecular polarizability.^{10,11} Since polarizability is a characteristic measure of physical size, this relationship implies that functional groups with larger polarizabilities enjoy more

* To whom correspondence should be addressed. Phone: (212) 854-4162. Fax: (212) 860-6988. E-mail: flynn@chem.columbia.edu.

[†] Work supported by the Joint Service Electronics Program (U.S. Army, Navy, and Air Force; DAAHO4-94-G0057) and the donors of the Petroleum Research Fund, administered by the American Chemical Society. Equipment support was provided by the National Science Foundation (Grants CHE-94-19465 and DMR-94-24296).

[‡] Marie Curie Postdoctoral Fellow sponsored by the American Association of University Women. Present address: Rohm and Haas Company, Research Laboratories, Spring House, PA 19477.

[§] Permanent address: Department of Chemistry, Calvin College, Grand Rapids, MI 49546.

(1) Binnig, G.; Rohrer, H.; Gerger, C.; Weibel, E. *Phys. Rev. Lett.* **1982**, *49*, 57.

(2) Binnig, G.; Rohrer, H. In *Trends in Physics*; Janta, J., Pantoflick, J., Eds.; European Physical Society: The Hague, 1984; pp 38–46.

(3) McGonigal, G. C.; Bernhardt, R. H.; Thomson, D. J. *Appl. Phys. Lett.* **1990**, *57*, 28.

(4) McGonigal, G. C.; Bernhardt, R. H.; Yeo, Y. H.; Thomson, D. J. *J. Vac. Sci. Technol., B* **1991**, *9*, 1107.

(5) Rabe, J. P.; Buchholz, S. *Science* **1991**, *253*, 424.

(6) Bard, A. J.; Fan, F. F.; Kwak, J.; Lev, O. *Anal. Chem.* **1989**, *61*, 132.

(7) Bard, A. J.; Dennault, G.; Lee, C.; Mandler, D.; Wipf, D. O. *Acc. Chem. Res.* **1990**, *23*, 357.

(8) Bard, A. J.; Unwin, P. R.; Wipf, D. O.; Zhou, F. In *AIP Conference Proceedings 241*; Wickramasinghe, H. K., Ed.; AIP Press: New York, 1992; p 235.

(9) Venkataraman, B.; Flynn, G. W.; Wilbur, J.; Folkers, J. P.; Whitesides, G. M. *J. Phys. Chem.* **1995**, *99*, 8684.

(10) Cyr, D. M.; Venkataraman, B.; Flynn, G. W.; Black, A.; Whitesides, G. M. *J. Phys. Chem.* **1996**, *100*, 13747.

(11) Cyr, D. M.; Venkataraman, B.; Flynn, G. W. *Chem. Mater.* **1996**, *8*, 1600.

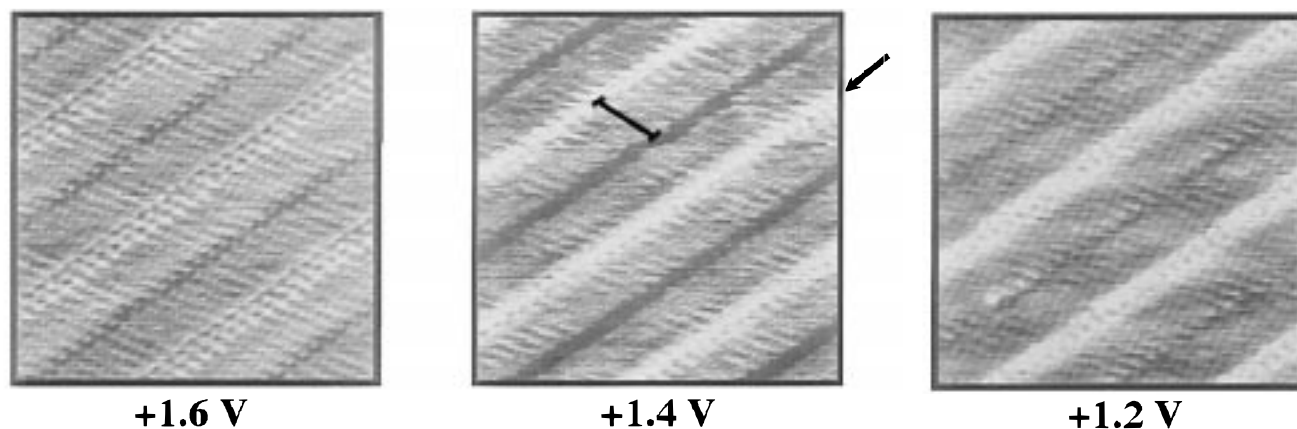


Figure 1. $10 \times 10 \text{ nm}^2$ scans of octadecanamide obtained at a setpoint current of 240 pA and the indicated bias voltage in constant-current mode. Lighter areas reveal topographically higher regions, while darker areas are indicative of topographically lower ones. The black bar denotes the width of one molecular row. The arrow in the image collected at +1.4 V indicates the position of the amide functional group. The images have been flattened using a zeroth-order polynomial in order to remove vertical offset between scan lines. No filtering has been performed.

favorable spatial overlap with the STM tip, resulting in augmented contrast. This model is also consistent with a tunneling mechanism proposed by Lang and co-workers¹² to explain the contrast observed for Xe on Ni(110). This contrast derives both from the spatial extent (*geometry*) of the electron density, which is pushed away from the Ni surface due to the presence of the Xe atom, and from a weak *electronic coupling* between Xe and Ni. The coupling arises from an off-resonant interaction between the perturbed Xe 6s level and the Ni Fermi level.

In this paper we use a simple tunneling spectroscopy methodology to record changes in constant-current topographs as a function of bias voltage for three functionalized hydrocarbons (section II). This method is similar to that employed by Hibino *et al.*¹³ in their study of the voltage dependence of image contrast for elaidic acid. The molecules considered here, octadecanamide, bromodocosane, and octadecyl sulfide, display remarkable contrast enhancement given the polarizability argument outlined above. For instance, the amide functionality exhibits an unusually large tunneling current despite its fairly small molecular polarizability ($5.7 \times 10^{-24} \text{ cm}^3$ for CH_3CONH_2),¹⁴ comparable to those of unsubstituted alkanes, alcohols, and chloroalkanes ($5.1 \times 10^{-24} \text{ cm}^3$);¹⁴ these functional groups exhibited little if any contrast variation in STM images.^{10,11} This would suggest that electronic factors (not surprisingly) also contribute significantly to the imaging mechanism. The collected images are described and analyzed in order to extract a quantitative measure of the topographic height of the functional group relative to the carbon chain at each voltage sampled (section III). Finally, the contributions that both *geometric factors* and *electronic coupling* make to the imaging of these hydrocarbons are explored in light of the various mechanisms which have been proposed for tunneling.

II. Experimental Section

All of the studies described here have been performed using a Nanoscope III scanning tunneling microscope (Digital Instruments) operating at the liquid–solid interface. Probes have been fabricated by mechanically snipping 0.25 mm diameter platinum/

rhodium (87/13) wire (Omega) at an acute angle in order to produce sharp tips; gold tips were also used in order to verify the generality of the results. Highly ordered pyrolytic graphite (HOPG) substrates (Advanced Ceramics, XZB grade) were freshly cleaved prior to imaging. A few microdroplets of the solution containing the derivatized hydrocarbon of interest were pipetted on to the HOPG, and the samples were mounted on the microscope.

Solutions were prepared by adding 1 mg of octadecanamide ($\text{CH}_3(\text{CH}_2)_{16}\text{CONH}_2$) or 1-bromodocosane ($\text{CH}_3(\text{CH}_2)_{21}\text{Br}$), both purchased from Aldrich, or octadecyl sulfide ($\text{CH}_3(\text{CH}_2)_{17}\text{S}(\text{CH}_2)_{17}\text{CH}_3$), synthesized as in ref 15, to 1 mL of phenyloctane. The solvent had been deaerated by bubbling N_2 through it for 10 min. The samples were then left to dissolve and thermally equilibrate for approximately 24 h prior to usage.

Height versus voltage measurements were obtained by sequentially varying the bias voltage, in 0.1 V increments, applied to the sample in the range from -1.6 to -0.6 and $+1.6$ to $+0.8$ V, while recording STM topographs as a function of tip height above the sample (constant-current mode). For these images, “brighter” portions correspond to topographically higher regions. The setpoint current was typically 240 pA, although data have been acquired at other current values to test the reproducibility of the results. Generally, at least four STM images were collected at each bias voltage to eliminate any spurious effects introduced by the scanning direction; also, images have been acquired on different days to confirm the generality of the results. All of the images shown are representative of the larger collection of data. Ratios of the measured topographic height of the functional group to the remaining carbon chain have been extracted from these images. (See below.)

III. Results

A. Octadecanamide. STM topographs of octadecanamide, bromodocosane, and octadecyl sulfide have been acquired over a range of bias voltages, as displayed in Figures 1, 2, and 3, respectively. As depicted in Figure 1, octadecanamide forms a two-dimensional thin-film comprised of molecules arranged in an all-trans configuration on the graphite surface. One molecular length, approximately 2.0 nm, is shown by the black bar in the image collected at +1.4 V (Figure 1). This value agrees well with that predicted for the length of an all trans molecular structure in which the distance between alternate methylene groups in the hydrocarbon backbone is 2.51 Å. The bright portion of each row (demarcated by the arrow in the image) indicates the position of the amide

(12) Eigler, D. M.; Weiss, P. S.; Schweizer, E. K.; Lang, N. D. *Phys. Rev. Lett.* **1991**, *66*, 1189.

(13) Hibino, M.; Sumi, A.; Hatta, I. *Jpn. J. Appl. Phys.* **1995**, *34*, 3354.

(14) *Handbook of Chemistry and Physics*, 71st ed.; CRC Press, Inc.: Boston, MA, 1990–91.

(15) Bain, C. D.; Troughton, E. B.; Tao, Y.-T.; Evall, J.; Whitesides, G. M.; Nuzzo, R. G. *J. Am. Chem. Soc.* **1989**, *111*, 321.

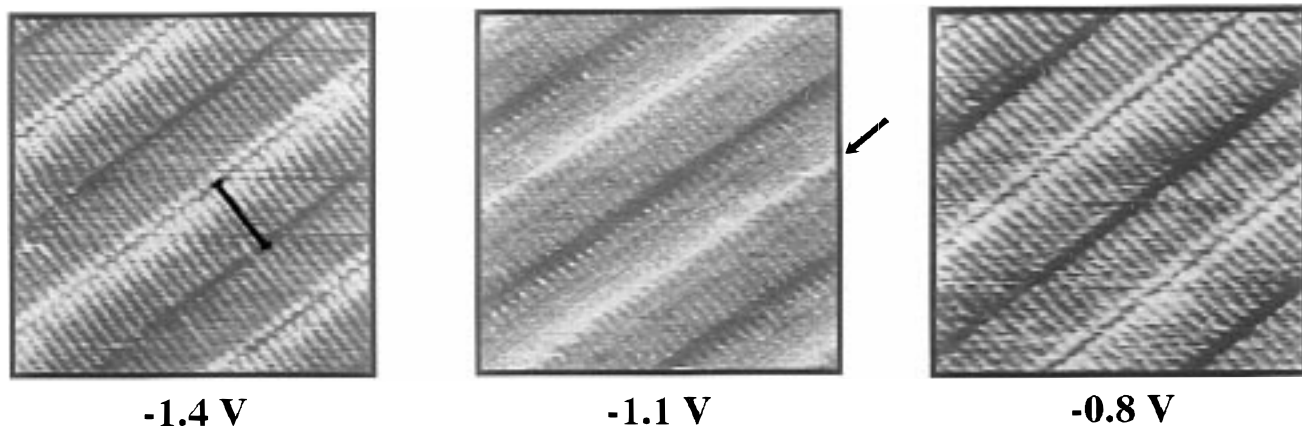


Figure 2. $10 \times 10 \text{ nm}^2$ topographs of 1-bromodocosane obtained at a setpoint current of 300 pA and the indicated bias voltage in constant-current mode. The black bar denotes the width of one molecular row (-1.4 V image). The arrow in the image collected at -1.1 V indicates the position of the bromide functional group. The images have been flattened using a zeroth-order polynomial in order to remove vertical offset between scan lines. No filtering has been performed.

($\text{O}=\text{C}-\text{NH}_2$) functional group. The molecules orient in a “head-to-head” configuration where the functional group of one molecule lies adjacent to the functional group of the next molecule. Moreover, the angle between the molecular axis and the trough has been measured as 68° , in accord with a preferential packing arrangement arising from the maximization of hydrogen-bonding interactions between the adjacent amide groups. These experimental observations are in good accord with those reported by Takeuchi *et al.*¹⁶ for the same molecule. Further, preliminary simulations using the Biosym molecular modeling package reveal that the preferred ordering of these molecules on a graphite substrate is dominated by strong hydrogen-bonding interactions, yielding a “head-to-head” configuration irrespective of the initial geometrical arrangement of molecules supplied to the modeling routine.

As shown in Figure 1, the highest bias voltage at which we have been able to collect data is $+1.6 \text{ V}$; attempts to image octadecanamide at higher voltages resulted in a loss of resolution. It is evident at this voltage that the amide functional group is readily visible, exhibiting enhanced contrast relative to both the hydrocarbon chain and the trough between molecular rows.

As the bias voltage is reduced to $+1.4 \text{ V}$, the relative tunneling probability of the amide group clearly increases, as revealed in the figure. Here, the contrast of the hydrocarbon chain has remained constant (compared to the $+1.6 \text{ V}$ image), while the troughs have darkened.

When the voltage is again lowered, in this case to $+1.2 \text{ V}$, the relative intensity of the amide group to the carbon atoms in the chain appears to have lessened, resulting in an overall contrast similar to the $+1.6 \text{ V}$ topograph. Further, the collected images display a moiré pattern. This pattern or intensity modulation is suggestive of a lack of registry (incommensurability) between the carbon chain of the molecule and the underlying graphite lattice; this phenomenon typically results in an interference pattern between the adsorbed molecules and the substrate. The moiré pattern persists down to the lowest voltages sampled.

At low bias voltages, $+0.8 \text{ V}$ for example, the height of the amide functional group and that of a representative carbon in the hydrocarbon chain are nearly equivalent. As the voltage is reduced even further, octadecanamide molecules are still visible to the microscope; however, little

distinction exists between the functionalized part of the molecule and the rest of the chain. At the lowest voltage investigated, $+0.05 \text{ V}$, only the underlying graphite is detected.

For images captured at negative bias voltages (tunneling from the sample to the tip), the same general trends are observed: the greatest contrast of the amide functional group is obtained at -1.4 V ; changes in voltage from this value result in decreased height of the amide group relative to the hydrocarbon chain; and at the very lowest voltages examined (between -0.8 and -0.1 V), no differentiation between the substituted end and the carbon chain is noticeable.

Images have also been collected at constant gap resistance ($R = V_{\text{bias}}/I_{\text{setpoint}}$, where $R = 4.67 \times 10^9 \Omega$) in order to insure that changes in functional group contrast do not derive from modifications in the tip-to-sample distance as V_{bias} has been varied. The images at constant resistance closely mimic those shown in Figure 1, suggesting that deviations in tip-sample displacement play a minimal role in these results.

B. Docosane Bromide. Images of docosane bromide collected at several bias voltages are presented in Figure 2. As described previously,^{10,11} the bromides lie in a “head-to-head” configuration with the bromide end groups of neighboring molecules adjacent to each other. The angle between one molecular axis and the trough dividing the lamellae has been measured as approximately 90° . Moreover, two conformations have been observed when imaging the bromides: in the first, the bromide end of the molecule appears “bright” (high) with respect to both the hydrocarbon backbone and the trough between rows of molecules; in the second, the bromide end is “dark” (low), exhibiting similar contrast to the trough. The difference between the two conformations has been tentatively attributed to a rotation of the terminal bromide functional group in and out of the plane of the molecular film. In the “bright” (high) orientation, the bromide group is tilted upward, out of the plane of the film, resulting in more favorable spatial overlap between the tip and the bromide terminal group; in the “dark” configuration, the bromide atom is pushed downward, residing within the molecular plane of the adsorbate.^{10,11} Because of this effect, we have been careful to obtain and analyze as a function of voltage only those images in which the bromide functional group appears high to the scanning tunneling microscope.

For docosane bromide the bias voltage has been varied from -1.5 to -0.6 V . At voltages above -1.5 V , no images

(16) Takeuchi, H.; Kawauchi, S.; Ikai, A. *Jpn. J. Appl. Phys.* **1996**, *35*, 3754.

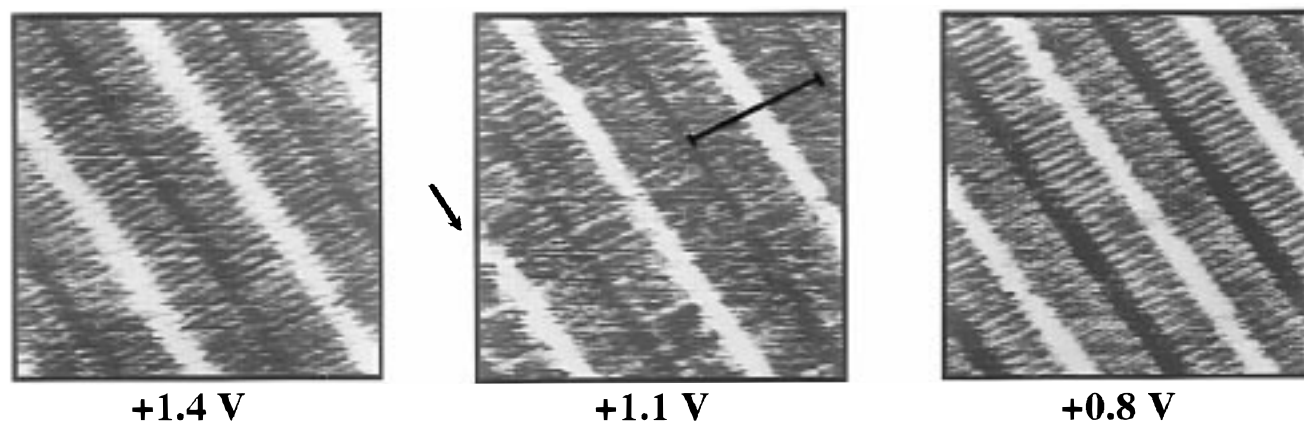


Figure 3. $10 \times 10 \text{ nm}^2$ images of octadecyl sulfide obtained at a setpoint current of 300 pA and the indicated bias voltage in constant-current mode. The black bar denotes the width of one molecular row. The arrow in the topograph collected at +1.1 V indicates the position of the sulfide functional group. The images have been flattened using a zeroth-order polynomial in order to remove vertical offset between scan lines. No filtering has been performed.

have been collected due to poor resolution. As depicted in Figure 2, the bromide end group (solid arrow) is clearly distinguishable from the hydrocarbon backbone. In contrast to the case for the amides, as the voltage is changed over the range sampled for docosane bromide (see, for instance, topographs acquired at -1.4 and -1.1 V), there is little, if any, qualitative alteration in the height of the bromide group relative to the carbon chain or the trough; i.e., bromine remains consistently high. This trend continues to -0.8 V, after which the height of the functional group decreases slightly; however, unlike the case for the amide molecule, the contrast of the functional group and that of the carbon backbone never become equal.

Attempts to capture and analyze images of docosane bromide at positive bias voltages have not met with much success in these studies. In particular, changes from negative to positive bias frequently appear to induce a transition in the contrast exhibited by the bromine terminal group in which the bromine atom presumably rotates from its out-of-plane high conformation to the in-plane low conformation. A possible alternative explanation is that the change in tunneling voltage polarity optimizes the electronic coupling among tip, surface, and adsorbate in such a way that the tunneling probability over the bromine atom is decreased.

C. Octadecyl Sulfide. For octadecyl sulfide, STM images have been captured in the range from $+1.5$ to $+0.7$ V, as shown in Figure 3. The two-dimensional thin film of octadecyl sulfide reveals hydrocarbon arms extended linearly from the sulfur atom positioned at the center of the molecule. The sulfide molecules align with their molecular axes (black bar) oriented at approximately 90° with respect to the troughs.

As with other sulfur-derivatized hydrocarbons (thiols and disulfides), the functionalized atom (S) in octadecyl sulfide exhibits markedly enhanced contrast compared to the hydrocarbon arms.^{9–11} For images obtained at the highest voltages, $+1.6$ to $+1.3$ V, the sulfide group appears twice as high as the backbone. At intermediate voltages in the range $+1.2$ to $+1.0$ V, the height increases slightly. This effect is not immediately discernible in the images, however, as the height of the sulfur atom appears to saturate the STM images. As the bias is again lowered, the contrast of the sulfur atom decreases slightly, yielding topographs that are very similar to those obtained at the highest voltages. Images observed at voltages below $+0.7$ V are not presented due to poor resolution, although it

should be noted that even at low bias voltages (e.g., $+0.1$ V) the sulfur atoms plainly stand out in the interfacial layer.

While octadecyl sulfide has been observed at the liquid–graphite interface at negative bias voltages, the images lacked both sufficient clarity and stability for a voltage dependence study to be conducted.

D. Analysis of Voltage Dependence of Functional Group Contrast. In order to evaluate the voltage dependence of the STM contrast for octadecanamide, bromodocosane, and octadecyl sulfide films in a more quantitative manner, we have performed a roughness analysis on the topographs. Each image has been flattened by using a zeroth order polynomial to remove vertical offset between scan lines. For the roughness analysis only a $10 \times 10 \text{ nm}^2$ portion of the flattened image has been considered. A small, square integration box (typical dimensions, length and width, 0.16 – 0.24 nm) is drawn over the amide, bromide, or sulfide functional group, and the mean height, an average over the heights of all of the points within the box, is recorded. The box is then moved across the *same* molecule and positioned above a representative carbon in the chain, where the height is again measured. The same molecule is analyzed to eliminate any experimental bias due to effects such as moiré patterns present in the topographs. Finally, the mean height is extracted at the trough. A minimum of eight heights have been recorded at each of the three positions for each image collected.

Given the highly mobile nature of the molecular thin films investigated here, a comparison of the measured topographic heights at the three positions indicated above as a function of bias voltage is not instructive; these individual values actually may vary from day to day within a data set collected at any one voltage. Instead, we calculate a ratio of the measured height at the position of the functional group relative to the carbon chain:

$$\frac{[\text{height}(\text{functional group}) - \text{background}]}{[\text{height}(\text{carbon chain}) - \text{background}]}$$

Here, the subtraction of the background, i.e. the height at the trough, normalizes the ratio for overall contrast variations (resulting from molecular motion, differences in the sharpness of the tunneling tips, etc.) among the STM scans. The value calculated for this ratio remains constant for a particular voltage over all the images collected. The results of this calculation for all three

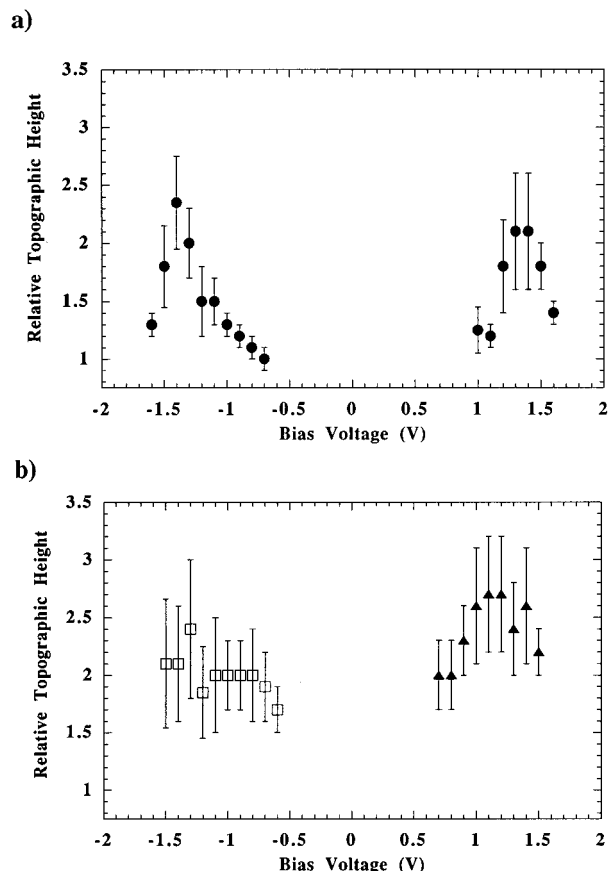


Figure 4. (a) Plot of the ratio of the measured topographic height of the amide functional group ($\text{O}=\text{C}-\text{NH}_2$) to that of a representative carbon atom in the hydrocarbon backbone versus bias voltage. The octadecanamide data are shown using solid circles. Error bars on the ratios reflect one standard deviation from the mean. (b) Plot of the ratio of the measured topographic height of the bromide (open squares) and sulfide (filled triangles) functional groups relative to that of a representative carbon in the hydrocarbon backbone versus bias voltage. Error bars on the ratios reflect one standard deviation from the mean.

substituted hydrocarbons, octadecanamide, bromodocosane, and octadecyl sulfide, are plotted in Figure 4 as a function of bias voltage. Error bars on the data points reflect one standard deviation from the mean of the relative height ratio.

As displayed by the solid circles in Figure 4a, peaks in the voltage dependence are present over the $\text{O}=\text{C}-\text{NH}_2$ group for octadecanamide around $|V| = 1.4$ V with a measured topographic height ratio greater than 2. Small shifts of ± 0.1 V from this value result in significant decreases in the relative height of the amide functional group compared to the hydrocarbon backbone. Larger changes from $|V| = 1.4$ V bring the ratio of the measured topographic height to its limiting value of 1, signifying equal contrast for both the amide group and the hydrocarbon chain. The full width at half maximum (fwhm) of the ratio of the height distribution is approximately 0.5 V.

In comparison, the image of docosane bromide shows a very flat voltage dependence (open squares in Figure 4b); the ratio of the measured topographic height of the bromide group to the carbon atoms in the chain remains fixed (within error bars), over nearly the entire voltage range sampled, at a value of approximately 2. The only exception to this occurs at -0.6 V, where the ratio decreases to 1.7; it should be noted, however, that (unlike octadecanamide) equal contrast between bromine and carbon has not been observed (ratio = 1).

Finally, the STM image of octadecyl sulfide (filled triangles in Figure 4b) exhibits a very weak voltage dependence. While the height data are not as strongly peaked as in the case of octadecanamide, the ratios are also not as flat as for the bromide molecules. Instead, a mild peak (fwhm ≈ 0.7 V) appears in the vicinity of 1.1 V; here, the ratio of the topographic height of the sulfur atom to the carbon chain has gradually risen from a value of 2.2 to approximately 2.7. Below 1.0 V, the sulfur ratio slowly tails off to 2.0. Again, for even the lowest voltages, the ratio never becomes 1, indicating that the sulfur atom is always clearly distinguishable from the remainder of the carbon chain.

IV. Discussion

As mentioned above, the tunneling mechanism for insulating molecules adsorbed on conductive surfaces is still the subject of great interest. Various mechanisms have been put forth to describe STM's ability not only to distinguish between the insulating adsorbates and the atoms of the surface but also to differentiate between atoms within the adsorbate. For the purposes of this discussion, these mechanisms will be loosely grouped into two broad categories, weak or strong (resonant tunneling) coupling on the basis of the degree of electronic coupling within the tip-adsorbate-substrate system.

Lang and co-workers have proposed that the contrast observed in STM images of Xe adsorbed on Ni(110) derives from a weak electronic coupling between the atomic levels of the adsorbate and the electronic states of the Ni substrate.¹² Here, the Xe atoms appear as 1.5 \AA protrusions within the STM topographs. To explain Xe's remarkable visibility in STM, Lang and co-workers¹² have used an adatom on "jellium" model to calculate the conduction electron density with and without the Xe present. The computations reveal that the Xe atom pushes electron density away from the Ni surface, resulting in favorable overlap between the tip and adsorbate, enabling the "insulating" atoms to be imaged successfully by STM. Further calculations demonstrate that Xe makes a significant contribution to the local density of states (LDOS), when the tip is far from the Ni surface. While this additional contribution to the LDOS is peaked approximately 0.5 eV below the Ni vacuum level, possessing a fwhm of 0.5 eV, it is the tail of the Xe LDOS distribution, which extends down to the Ni Fermi level, that results in the weak electronic coupling to the surface. This has been suggested as the mechanism or pathway leading to the heightened contrast over the Xe atom obtained for this system.

Xe on Ni(110) serves as the atomic analog to the insulating organic molecules physisorbed on HOPG studied here. For both systems there exists a large gap between the highest occupied and the lowest unoccupied orbitals, amounting to 8–12 eV. Due to this large energy difference, it is reasonable to assume weak nonresonant coupling between the electronic levels of the graphite substrate and the highest occupied and lowest unoccupied molecular orbitals (HOMO's and LUMO's) of the adsorbate. Despite the weak electronic coupling, the spatial extent of the electron density for the combined adsorbate-substrate system is pushed away from the substrate because of the physical position of the adsorbate on the surface. In these cases, the STM image is expected to reflect the shape of the adsorbate HOMO or LUMO overlapped by the wave function of the tip atom(s). Here, *geometry* will generally be the predominating factor in the tunneling mechanism.

This type of geometry-determined tunneling mechanism seems to govern the images collected for docosane bromide. The very flat voltage dependence (Figure 4b) suggests that the electronic energy levels of the adsorbate play a minimal role in the differentiation between the terminal bromide group and the carbon backbone. Instead, it seems likely that the favorable spatial overlap (geometry) imposed by an orientation in which the bromine functional group appears raised relative to the rest of the molecule controls its discrimination by STM. Similar to the Xe on Ni case, a small amount of electronic coupling must exist for the bromide to be imaged; however, in the vicinity of the Fermi level, it is presumed that any addition to the LDOS contributed by docosane bromide is relatively constant as a function of energy (voltage). It should be noted, however, that the exact placement of the frontier orbital levels (i.e. the HOMO and LUMO) for this bromide derivatized hydrocarbon remains unknown, precluding a direct assessment of the degree of adsorbate–substrate coupling at the present time. Still, a geometry-driven tunneling mechanism would also explain the lack of contrast exhibited by the functional group in the second configuration observed for the two-dimensional interfacial layer in which the Br group appears dark relative to the hydrocarbon chain.^{10,11} Further, increased tunneling probability based upon molecular geometry is consistent with the hypothesis proposed previously^{10,11} in which height in STM images correlates with a large molecular polarizability (for $\text{CH}_3\text{CH}_2\text{Br}$, $\alpha = 8.05 \times 10^{-24} \text{ cm}^3$).¹⁴

In contrast to the case for 1-bromodocosane, the peak exhibited in the voltage dependent results for octadecanamide (Figure 4a) suggests a strong electronic coupling between adsorbate and substrate, hinting at a resonant tunneling mechanism. Resonant tunneling has been proposed as the dominant tunneling mechanism for a number of systems, including 4-octyl-4'-cyanobiphenyl¹⁷ and isolated DNA strands.¹⁸ In these cases, a strong interaction exists between the electronic energy levels of the adsorbate and those of either the substrate or the tip, which may mediate electron tunneling between the tip and the surface. The molecular levels of the adsorbate act as intermediate states during the electron tunneling process and increase tunneling conductance in the vicinity of the molecular adsorbate. Recently, Tao¹⁹ observed resonant tunneling by using electrochemical STM to “tune” the Fermi level of a graphite surface into resonance with an electronic level of iron(III) porphyrin. His voltage dependent measurements are very similar to those reported here.

Let us consider which electronic levels of octadecanamide are available for coupling to the graphite substrate and their degree of interaction. Following the prescription given by Ou-Yang *et al.*,²⁰ the energy levels of the adsorbate can be cataloged relative to those of the graphite surface and the Pt tip by defining a zero of energy as that level at which the electron can be effectively removed from the graphite surface or molecule. These correspond to the vacuum level and the ionization potential, respectively. Taking the substrate first and using the work function for graphite ($\phi = 4.7 \text{ eV}$), the Fermi level is positioned 4.7 eV below the zero of energy. Next, using the ionization

potential for octadecanamide (11 eV),²¹ the HOMO is placed -11 eV from the graphite vacuum level and 6.3 eV below the Fermi level. The HOMO–LUMO gap determines where the LUMO lies with respect to the graphite levels; Ikai and co-workers²¹ have calculated that this gap is approximately 16.8 eV. This sets the LUMO at +5.8 and +10 eV relative to the graphite vacuum and Fermi levels, respectively. Since the values computed for the ionization potential and HOMO–LUMO gap correspond to those for octadecanamide in the gas phase, the molecular levels of the adsorbed molecule should lie slightly lower in energy. Assuming a heat of adsorption of 1.2 eV (on the basis of the number of methylene units in the hydrocarbon chain),^{22,23} the LUMO is still separated by 4.6 eV from the vacuum level and even more from the Fermi level.

Given that these frontier orbitals are far removed from the surface Fermi level, it seems unlikely from an energetic standpoint that they can play a pronounced role in *resonant* electronic coupling, which might be expected to be responsible for the peak in the ratio of the topographic height as the voltage is varied. Instead, the HOMO and LUMO are expected to have a weak interaction with the graphite, similar to that of bromine, as discussed above.

Despite the energetically weak coupling between the substrate and molecular adsorbate HOMO and LUMO levels, the shape of the orbitals may still contribute to the contrast observed in the STM images, much like the case of Xe on Ni.¹² For instance, Sautet and Bocquet²⁴ have calculated that the orbitals of benzene which lie very far (tens of electronvolts) from a Pt(111) surface Fermi level make a significant contribution to the STM image, giving rise to the shape of the contours seen in the experimental topographs. Further, Claypool *et al.*²⁵ argue that orbital diffuseness occupies a prominent role in defining the overall electronic coupling matrix elements. Our images for octadecanamide (especially around $|V| = 1.4 \text{ V}$) appear to be in general accord with the molecular orbital shapes calculated by Ikai and co-workers.¹⁶ Like the STM topographs, diagrammatic representations of the computed HOMO and LUMO reveal localization of the wave function over the terminal amide ($\text{O}=\text{C}-\text{NH}_2$) group. The next lower HOMO (HOMO -1) and next higher LUMO (LUMO $+1$) show the wave function extending into the hydrocarbon chain away from the functional group.

While the calculated shapes of the molecular orbitals for octadecanamide are consistent with the overall picture of increased tunneling over the position of the amide functional group, they do not explain an increase in topographic height ratio as the energy (voltage) is tuned. The energy of the amide HOMO and LUMO levels relative to that of the graphite electronic states implies that they should be only weakly (off-resonantly) coupled to the graphite Fermi level. The molecular orbitals and the energy level diagram constructed thus far do not seem to adequately explain a peak or “resonance” in the voltage dependence at $|V| = 1.4 \text{ V}$. Instead, we speculate that other types of electronic levels of the adsorbate, including low-lying triplet levels²⁶ and negative ion states,^{27–30} may give rise to the changes in the STM images as the bias

(17) Mizutani, W.; Shigeno, M.; Ohmi, M.; Sugino, M.; Kajimura, K.; Ono, M. *J. Vac. Sci. Technol., B* **1991**, *9*, 1102.

(18) Mizutani, W.; Shigeno, M.; Sakakibara, Y.; Kajimura, K.; Ono, M.; Tanishima, S.; Ohno, K.; Tushima, N. *J. Vac. Sci. Technol., A* **1990**, *8*, 675.

(19) Tao, N. J. *Phys. Rev. Lett.* **1996**, *76*, 4066.

(20) Ou-Yang, H.; Marcus, R. A.; Källébring, B. *J. Chem. Phys.* **1994**, *100*, 7814.

(21) Kawauchi, S.; Muta, H.; Takeuchi, H.; Ikai, A. *International Conference on Scanning Tunneling Microscopy 4*, Kanagawa, Japan, 1996.

(22) Groszek, A. J. *J. Proc. R. Soc. London* **1970**, *314*, 473.

(23) Findenegg, G. H. *J. Chem. Soc., Faraday Trans.* **1973**, *69*, 1069.

(24) Sautet, P.; Bocquet, M.-L. *Phys. Rev. B* **1996**, *53*, 4910.

(25) Claypool, C. L.; Faglioni, F.; Goddard, W. A., III; Gray, H. B.; Lewis, N. S.; Marcus, R. A. *J. Chem. Phys. B* **1997**, *101*, 5978.

(26) Herzberg, G. *Electronic Spectra of Polyatomic Molecules*; Van Nostrand Reinhold Company: New York, 1966.

voltage is smoothly varied. Finally, it is also worth noting that the effects of the considerable electrical fields at the tip-adsorbate-surface interface can significantly impact on the coupling between surface Fermi levels and adsorbate HOMO-LUMO levels. Such an effect may be responsible for the relatively rapid change in topographic height observed as a function of voltage in the octadecanamide system.

V. Summary

Using STM, images of electrically insulating thin films of substituted long-chain hydrocarbons adsorbed on graphite have been successfully obtained with, in many cases, atomic resolution. Further, certain chemically

specific functional groups can be distinguished from the hydrocarbon backbone due to an increase in the tunneling probability in the STM images at the substituted positions. Finally, voltage dependent studies of the image contrast observed for octadecanamide, docosane bromide, and octadecyl sulfide suggest that participation of *geometric* and *electronic structure* factors can be distinguished. For docosane bromide, *topographic factors* appear to dominate the tunneling mechanism; while for octadecanamide, evidence for *resonant tunneling*, implying a strong electronic interaction, is suggested by the voltage dependent images.

Acknowledgment. The work described here benefited greatly from the encouragement and scientific insight of our colleague and friend Brian Bent. His presence at Columbia will be sorely missed. We gratefully acknowledge the assistance of Professor George Whitesides and Andrew Black at Harvard University, who supplied the samples of octadecyl sulfide. We also thank Seth Rubin for his helpful assistance in carrying out a number of experiments.

LA9707181

(27) Wentworth, W. E.; Geroge, R.; Keith, H. *J. Chem. Phys.* **1969**, *51*, 1791.

(28) Blaunstein, R. P.; Christophorou, L. G. *J. Chem. Phys.* **1968**, *49*, 1526.

(29) Ukraintsev, V. A.; Long, T. J.; Harrison, I. *J. Chem. Phys.* **1992**, *96*, 3957.

(30) Ukraintsev, V. A.; Long, T. J.; GowI, T.; Harrison, I. *J. Chem. Phys.* **1992**, *96*, 9114.